Magnetostructural Correlations for Hexachlorodicuprate(II) Salts: Crystal Structure and Magnetic Properties of the Tetrameric Complex $[\{Cu_2(terpy)Cl_4\}_2]$ (terpy = 2,2′:6′,2″-Terpyridine)†

José-Vicente Folgado, Pedro Gomez-Romero, Fernando Sapiña, and Daniel Beltrán-Porter*
UIBCM, Departament de Química Inorgànica, Universitat de València, Dr. Moliner 50, 46100 Burjassot, València, Spain

The crystal structure of the complex $[\{Cu_2(terpy)Cl_4\}_2]$ (terpy = 2,2′:6′,2″-terpyridine) has been determined. It crystallizes in space group $P\bar{1}$, $a = 11.136(7)$, $b = 8.365(4)$, $c = 9.263(5)$ Å, $\alpha = 97.13(5)$, $\beta = 93.60(5)$, $\gamma = 88.82(5)°$ and $Z = 2$. Least-squares refinement of 2 591 reflections with $I > 3\sigma(I)$ and 218 parameters gave a final $R = 0.070$ and $R' = 0.074$. The structure consists of discrete neutral tetrameric units formed by slightly bifolded $[Cu_2Cl_6]^{2-}$ dimers stacked between two planar $[Cu(terpy)Cl]^+$ entities. The co-ordination geometry around each copper ion can be described as tetragonal square pyramidal. Temperature-dependent e.s.r. spectra and magnetic susceptibility measurements have been reinterpreted on the basis of the tetrameric nature of the compound. Exchange coupling parameters of $J_{12}/k = -13 \pm 1$ K and $J_{23}/k = -68 \pm 2$ K have been estimated. The strength of the exchange interaction in the $[Cu_2Cl_6]^{2-}$ units is discussed on the basis of the structural features and compared with other bifolded systems, confirming the correlation of J with the bifold angle.

Significant progress has been made in the understanding of exchange interactions in the last several years,[1] and some relationships between magnetic properties and structural factors have been elucidated.[2] In this context, we have recently reported the synthesis and magnetic characterizaton of a wide set of copper(II) compounds containing $Cu(L_{III})X$ entities where L_{III} is a tridentate rigid quasi-planar N-donor ligand such as terpy (2,2′:6′,2″-terpyridine), pyridine-2-carbaldehyde 2′-pyridylhydrazone, 2,4,6-tris(2-pyridyl)-1,3,5-triazine, or *N*-(2′-pyridylcarbonylpyridinecarboximidate and X = halide, pseudohalide, hydroxide, or one half of a doubly charged bridging anion such as oxalate or chloranilate (2,5-dichloro-3,6-dihydroxy-*p*-benzoquinonate).[3–11] These moieties are bridged by the X anions to give dimers or more extended magnetic systems such as linear or ladder-like chains.[3–11]

Halogenocuprates(II) have been the subject of a great number of studies in recent years owing to the different geometries that they can adopt and the important role they play in several fields of current research in inorganic chemistry.[12–15] The compounds of formula $A[CuX_3]$, where X = Cl or Br and A is an organic or inorganic cation, can contain: (*i*) isolated $[Cu_nX_{3n}]^{n-}$ oligomers, (*ii*) stacked $[Cu_2X_6]^{2-}$ dimers, or (*iii*) $[CuX_3]^-$ linear chains. The $[Cu_2X_6]^{2-}$ dimers can be planar, twisted, or bifolded.[12] Bifold distortion is characterized by the angle σ between the bridging Cu_2X_2 planes and the terminal CuX_3 planes, whereas the twist distortion τ is defined by the angle between the central Cu_2X_2 and the terminal CuX_2 planes. The planar dimers usually form stacks with the copper(II) ions in a '4 + 2' co-ordination geometry, although isolated planar dimers have been recently reported.[12,16] The twisted dimers are isolated with distorted (flattened) tetrahedral copper(II) co-ordination mode, whereas the bifolded dimers form alternating chains with a '4 + 1' co-ordination geometry. For the planar dimers, increase of the bridging angle θ increases the antiferromagnetic coupling between the copper(II) ions, whereas the increase of the bifold angle σ favours ferromagnetic behaviour.[12–15]

We have reported the synthesis, spectroscopic and magnetic properties of the complex $Cu_2(terpy)Cl_4$ in the polycrystalline state.[10] Based on e.s.r. and magnetic results, the presence of two dimeric moieties, identified as $[\{Cu(terpy)Cl\}_2]^{2+}$ and $[Cu_2Cl_6]^{2-}$ was proposed. Only recently has it been possible to obtain single crystals suitable for *X*-ray structure determination. In this paper, the crystal structure of the complex is reported and the magnetic susceptibility measurements and e.s.r. spectra are reinterpreted in the light of the tetrameric nature of the compound, which contains slightly bifolded $[Cu_2Cl_6]^{2-}$ dimers stacked between two planar $[Cu(terpy)Cl]^+$ entities. Their magnetic properties are compared to those previously reported for other planar and bifolded $[Cu_2Cl_6]^{2-}$ dimers.

Experimental

Preparation of the Complex.—The compound $[\{Cu_2(terpy)Cl_4\}_2]$ was prepared from ethanolic solutions of $CuCl_2 \cdot 2H_2O$ and terpy following the procedure previously described.[10] Crystals suitable for *X*-ray structure determination were grown by slow evaporation of warm nitromethane solutions. They grew as fragile thin platelets exhibiting pleochroism, green or brown with unpolarized light depending on their orientation with respect to the light source.

Crystal Structure Determination.—*Crystal data.* Green-brown dichroic crystals of $C_{15}H_{11}Cl_4Cu_2N_3$, $M = 501.9$, triclinic, space group $P\bar{1}$, $a = 11.136(7)$, $b = 8.365(4)$, $c = 9.263(5)$ Å, $\alpha = 97.13(5)$, $\beta = 93.60(5)$, $\gamma = 88.82(5)°$, $U = 854.4(1)$ Å^3, $Z = 2$, $D_c = 1.951$ g cm^{-3}, $F(000) = 496$, $\mu(Cu\text{-}K_\alpha) = 86.4$ cm^{-1}.

Data collection. Preliminary cell dimensions and the space group were obtained from Weissenberg and oscillation photographs. The cell dimensions were refined from the setting angles of 25 reflections ($10 < 2\theta < 30°$) of a crystal mounted at room

---

† Hexa-μ-chloro-1:2κ^4*Cl*; 2:3 κ^4*Cl*; 3:4κ^4*Cl*-dichloro-2κ*Cl*,3κ*Cl*-bis(2,2′:6′,2″-terpyridine)-1κ^3*N*,4κ^3*N*-tetracopper(II).

Supplementary data available: see Instructions for Authors, *J. Chem. Soc., Dalton Trans.*, 1990, Issue 1, pp. xix—xxii.

Table 1. Fractional atomic co-ordinates (× 10^4) for $[\{Cu_2(terpy)Cl_4\}_2]$ with estimated standard deviations (e.s.d.s) in parentheses

Atom	*X/a*	*Y/b*	*Z/c*
Cu(1)	1 306(1)	−207(1)	1 074(1)
Cu(2)	2 919(1)	3 288(1)	2 753(1)
Cl(1)	−596(1)	1 033(2)	1 245(2)
Cl(2)	1 746(1)	820(1)	3 392(1)
Cl(3)	2 878(1)	−1 910(1)	931(1)
Cl(4)	2 624(1)	2 703(1)	353(1)
N(1)	4 513(3)	2 144(4)	3 064(4)
N(2)	3 294(3)	4 055(4)	4 789(4)
N(3)	1 611(3)	4 962(4)	3 116(4)
C(1)	5 092(4)	1 204(5)	2 062(5)
C(2)	6 164(4)	403(6)	2 381(5)
C(3)	6 610(4)	581(6)	3 829(5)
C(4)	6 006(4)	1 516(5)	4 884(5)
C(5)	4 972(3)	2 302(5)	4 467(5)
C(6)	4 252(4)	3 389(5)	5 473(4)
C(7)	4 473(4)	3 801(5)	6 966(4)
C(8)	3 685(5)	4 887(6)	7 725(5)
C(9)	2 710(4)	5 561(5)	6 976(4)
C(10)	2 550(4)	5 099(4)	5 496(4)
C(11)	1 596(4)	5 682(5)	4 481(5)
C(12)	742(4)	6 884(5)	4 891(5)
C(13)	−71(4)	7 347(6)	3 826(6)
C(14)	−50(4)	6 633(6)	2 424(6)
C(15)	814(4)	5 412(6)	2 098(5)

Table 2. Selected bond distances (Å) and angles (°) in the complex $[\{Cu_2(terpy)Cl_4\}_2]$ with e.s.d.s in parentheses

Cu(1)–Cl(1)	2.344(1)	Cu(2)–N(1)	2.021(4)
Cu(1)–Cl(2)	2.239(1)	Cu(2)–N(2)	1.938(3)
Cu(1)–Cl(3)	2.234(1)	Cu(2)–N(3)	2.014(3)
Cu(1)–Cl(4)	3.033(1)	Cu(2)–Cl(2)	2.613(1)
Cu(1)–Cl(1′)	2.271(1)	Cu(2)–Cl(4)	2.221(1)
Cl(1)–Cu(1)–Cl(2)	88.3(1)	Cl(2)–Cu(2)–Cl(4)	95.5(1)
Cl(1)–Cu(1)–Cl(3)	166.7(1)	N(1)–Cu(2)–Cl(2)	91.3(1)
Cl(2)–Cu(1)–Cl(3)	95.4(1)	N(1)–Cu(2)–Cl(4)	99.7(1)
Cl(1)–Cu(1)–Cl(4)	96.7(1)	N(2)–Cu(2)–Cl(2)	92.4(1)
Cl(2)–Cu(1)–Cl(4)	84.3(1)	N(1)–Cu(2)–Cl(4)	172.1(1)
Cl(3)–Cu(1)–Cl(4)	96.4(1)	N(1)–Cu(2)–N(2)	80.2(1)
Cl(1)–Cu(1)–Cl(1′)	83.1(1)	N(3)–Cu(2)–Cl(2)	97.7(1)
Cl(2)–Cu(1)–Cl(1′)	171.4(1)	N(3)–Cu(2)–Cl(4)	99.5(1)
Cl(3)–Cu(1)–Cl(1′)	93.1(1)	N(1)–Cu(2)–N(3)	157.8(1)
Cl(4)–Cu(1)–Cl(1′)	95.9(1)	N(2)–Cu(2)–N(3)	79.3(1)
Cu(1)–Cl(2)–Cu(2)	95.3(1)	Cu(1)–Cl(4)–Cu(2)	84.9(1)

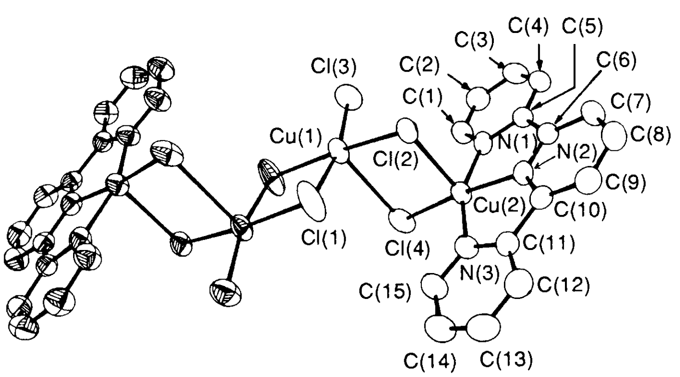

Figure 1. Perspective view and atomic numbering for $[\{Cu_2(terpy)Cl_4\}_2]$

temperature on a Phillips PW 1100 automatic diffractometer with Cu-K_α monochromated radiation. A total of 2 901 unique reflections were collected ($-13 \leqslant h \leqslant 13$, $-9 \leqslant k \leqslant 9$, $0 \leqslant l \leqslant 10$), with the variable-speed ω—2θ technique, of which 2 591 had $I > 3\sigma(I)$. Lorentz and polarization corrections were applied to the data, but not for absorption.

Structure solution and refinement. The structure was solved by direct methods (MULTAN 84),[17] showing initially the positions of all Cu and Cl atoms. A statistical test indicated centrosymmetry, and the space group $P\bar{1}$ was later confirmed during the refinement of the structure. The terpy ligand was located frrom successive Fourier difference syntheses. The model obtained was refined with the SHELX 76 system[18] by weighted anisotropic full-matrix least-squares methods. After refinement of positional and anisotropic thermal parameters for all non-hydrogen atoms, difference maps indicated the positions of all the hydrogen atoms; their positions were calculated and included as a fixed contribution to F_c. At convergence the final R factor was 0.070, and $R' = 0.074$ (218 parameters refined); $\Sigma w(|F_o| - |F_c|)^2$ was minimized where $w = 1/[\sigma^2(F_o) + 0.029\,344\,(F_o)^2]$ with $\sigma^2(F_o)$ from counting statistics. Only a few peaks very close to Cu atoms were apparent above the noise level in a final Fourier difference map.

Scattering factors and corrections for anomalous dispersion were taken from ref. 19. The geometrical calculations were performed with XANADU[20] and molecular illustrations were drawn with ORTEP.[21]

Additional material available from the Cambridge Crystallographic Data Centre comprises H-atom co-ordinates, thermal parameters, and remaining bond lengths and angles.

Physical Measurements.—Infrared, electronic, and *X*-band e.s.r. spectra, as well as magnetic susceptibility measurements, have been reported previously.[10] Variable-temperature *Q*-band e.s.r. spectra were recorded on a Varian E15 spectrometer.

Results and Discussion

Crystal Structure.—Final atomic co-ordinates for all non-hydrogen atoms are listed in Table 1. Figure 1 shows a perspective view of the molecule with the atomic numbering scheme. Selected bond distances and angles are listed in Table 2. The crystal structure consists of discrete tetrameric units. Two Cu(terpy)Cl groups are located at the ends of the tetramer, and are bridged by an almost planar Cu_2Cl_6 moiety, the centre of which sits on a centre of inversion (Figure 1).

All Cu atoms are subject to a distorted square-pyramidal co-ordination with typically long axial bonds. The basal Cu(1)–Cl distances, ranging from 2.234(1) to 2.344(1) Å, are similar to those found in related chlorocuprates,[12–16] whereas the axial Cu(1)–Cl(4) bond is considerably longer [3.033(1) Å]. The four equatorial chlorine atoms are nearly coplanar with deviations from the least-squares plane smaller than ±0.13 Å; Cu(1) lies 0.13 Å from this plane. The co-ordination geometry around Cu(2) is very similar to that reported for the compound $[Cu(terpy)Cl]_2[PF_6]_2$.[8] The basal atoms [Cl(4)N(1)N(2)N(3)] lie practically on a plane with deviations no greater than 0.02 Å from the least-squares plane, whereas the Cu(2) atom is 0.16 Å away from this plane. Both basal planes are almost parallel, the dihedral angle between them being only 8.7°.

The Cu_2Cl_6 units cannot be considered strictly planar since the atoms show deviations as large as 0.17 Å from the least-squares plane. Notwithstanding, the twist angle τ, defined as between the Cu(1)Cl(1)Cu(1′)Cl(1′) and the Cu(1)Cl(2)Cl(3) planes, is only 12.8°. On the other hand, the bifold distortion, characterized by the angle σ between Cu(1)Cl(1)-Cu(1′)Cl(1′)Cl(2)Cl(2′) and the Cu(1)Cl(1)Cl(2)Cl(3) planes, is 12.4°. The bridging angle θ is 97.0(1)° and the Cu(1) ··· Cu(1′) distance is 3.456(1) Å.

Lastly, it is to be noted that the double chloride bridge between Cu(1) and Cu(2) is quite asymmetric, with Cu(1)–Cl(4)

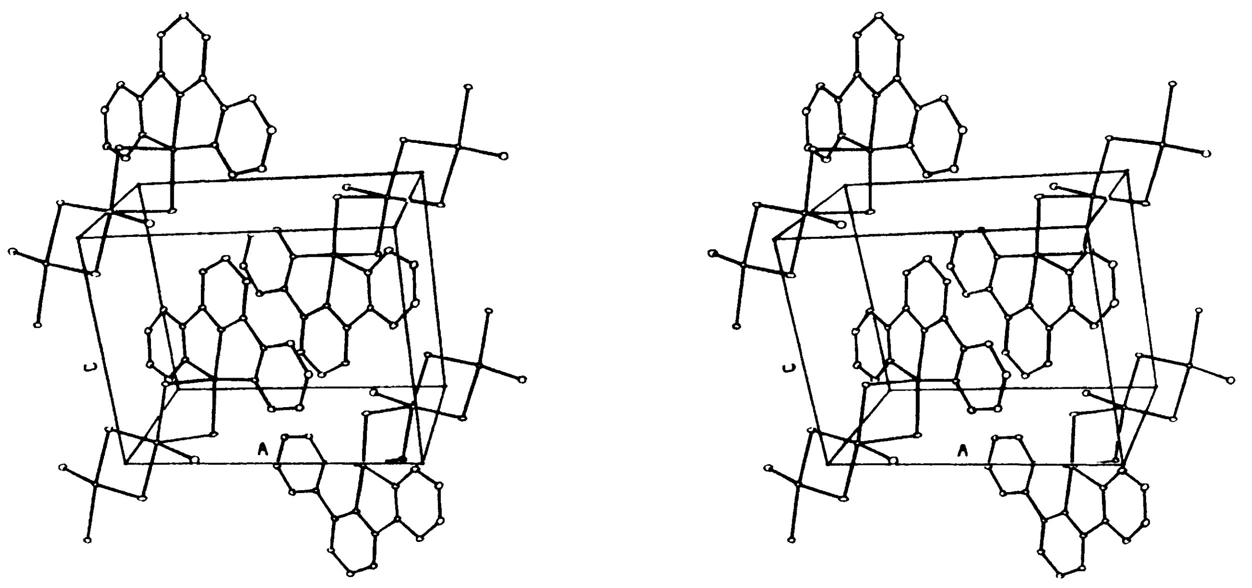

Figure 2. Stereoscopic view of the unit cell for $[\{Cu_2(terpy)Cl_4\}_2]$

and Cu(2)–Cl(2) distances of 3.033(1) and 2.613(1) Å, respectively, and Cu(1)–Cl(2)–Cu(2) and Cu(1)–Cl(4)–Cu(2) bridging angles of 95.3(1) and 84.9(1)°, respectively. The Cu(1) ⋯ Cu(2) distance is 3.595(1) Å.

Figure 2 shows the packing of tetramers within the unit cell and the close proximity of neighbouring aromatic ligands. The distance between the terpy plane and the closest centre of inversion is 1.669 Å, implying a separation of neighbouring terpy planes of 3.338 Å.

Magnetism and E.S.R. Spectroscopy.—The magnetic behaviour of this compound in the temperature range 4—280 K was previously reported by two of us.[10] Curie–Weiss behaviour is observed above 40 K corresponding to $C = 0.36$ and $\Theta = -60$ K, whereas below 40 K a change of slope arises with $C = 0.18$ and $\Theta = -3$ K. The effective magnetic moment per Cu^{II} decreases continuously from 1.84 μ_B at 280 K to 1.26 μ_B at 30 K, stays practically constant from 30 to 20 K, then decreases and tends to zero on further cooling (1.13 μ_B at 4 K). These results suggest that half of the copper(II) ions are strongly antiferromagnetically coupled, so that at low temperature only the other half contribute to the magnetic moment. Furthermore, the small Θ value in this temperature range suggests a weak antiferromagnetic coupling between these copper(II) ions. On the basis of these facts the observed behaviour was satisfactorily fitted assuming the existence of two independent dimers, namely $[\{Cu(terpy)Cl\}_2]^{2+}$ and $[Cu_2Cl_6]^{2-}$, and the following set of parameters: $J_1/k = -2$ K, $g_1 = 2.09$, $J_2/k = -78$ K, and $g_2 = 2.26$. However, in the light of the tetrameric arrangement found in this compound, both e.s.r. and magnetic results must be reinterpreted.

The Hamiltonian for a tetrameric system can be written, avoiding anisotropic and antisymmetric exchange terms, as equation (1) where, in our case, $J_{12} = J_{34}$ is the exchange

$$\hat{H} = -2J_{12}\hat{S}_1\hat{S}_2 - 2J_{23}\hat{S}_2\hat{S}_3 - 2J_{34}\hat{S}_3\hat{S}_4 \qquad (1)$$

constant between the outer pair of copper(II) ions, and J_{23} is the central exchange constant. This model has been solved exactly elsewhere and the expression for the magnetic susceptibility has been given, assuming that the Lande factors for all the copper(II) atoms are the same.[22] When we tried to fit our experimental data to this expression, no reasonable fit was obtained. The discrepancies obviously arise from the last assumption, since in our case the Lande factors for Cu(1) and Cu(2) must be different. We have developed a model for this system starting from the eigenvalues and eigenfunctions for the Hamiltonian (1). Considering the Zeeman Hamiltonian (2) as a perturbation

$$\hat{H} = \mu_B H[g_1(\hat{S}_1^z + \hat{S}_4^z) + g_2(\hat{S}_2^z + \hat{S}_3^z)] \qquad (2)$$

in our model, we obtained the first-order corrections for the energy, defining an effective Lande factor for each spin state. The energy levels, spin quantum numbers and effective g values are given below.

$S_1 = 2$ $E_1 = -J_{12} - (J_{23}/2)$ $g_1^* = (g_1 + g_2)/2$
$S_2 = 1$ $E_2 = J_{12} - (J_{23}/2)$ $g_2^* = (g_1 + g_2)/2$
$S_3 = 1$ $E_3 = J_{23}/2 + (J_{12}^2 + J_{23}^2)^{\frac{1}{2}}$ $g_3^* = g_1c_{2-}^2 + g_2c_{1-}^2$
$S_4 = 1$ $E_4 = J_{23}/2 - (J_{12}^2 + J_{23}^2)^{\frac{1}{2}}$ $g_4^* = g_1c_{2+}^2 + g_2c_{1+}^2$
$S_5 = 0$ $E_5 = J_{12} + (J_{23}/2) + (4J_{12}^2 - 2J_{12}J_{23} + J_{23}^2)^{\frac{1}{2}}$
$S_6 = 0$ $E_6 = J_{12} + (J_{23}/2) - (4J_{12}^2 + 2J_{12}J_{23} + J_{23}^2)^{\frac{1}{2}}$

$$c_{1\pm} = [1/(1 + K_{\pm}^2)]^{\frac{1}{2}}, c_{2\pm} = K_{\pm}c_{1\pm}$$
$$K_{\pm} = [-J_{23} \pm (J_{12}^2 + J_{23}^2)^{\frac{1}{2}}]/J_{12}$$

The expression for the tetramer magnetic susceptibility is then obtained by means of the van Vleck formula, and is given by equation (3) where Z is the partition function defined in equation (4).

$$\chi_mT = (N_0\mu_B^2/k)[10(g_1^*)^2\exp(-E_1/kT) + 2(g_2^*)^2\exp(-E_2/kT) + 2(g_3^*)^2\exp(-E_3/kT) + 2(g_4^*)^2\exp(-E_4/kT)]/Z \qquad (3)$$

$$Z = 5\exp(-E_1T) + 3\exp(-E_2/kT) + 3\exp(-E_3/kT) + 3\exp(-E_4/kT) + \exp(-E_5/kT) + \exp(-E_6/kT) \qquad (4)$$

By using this model, a satisfactory fit of the experimental data has been obtained with the following parameters: $J_{12}/k = -13 \pm 1$ K, $J_{23}/k = -68 \pm 2$ K, $g_1 = 2.05 \pm 0.01$, and $g_2 = 2.32 \pm 0.03$ (Figure 3).

The energy-level diagram given in Figure 4 has been drawn based on this set of parameters. Using such a diagram we can now understand the temperature dependence of the e.s.r. spectra. Both the *X*- and *Q*-band spectra recorded at 4.2 K show a narrow axial signal leading to $g_{\parallel} = 2.22$ and $g_{\perp} = 2.05$

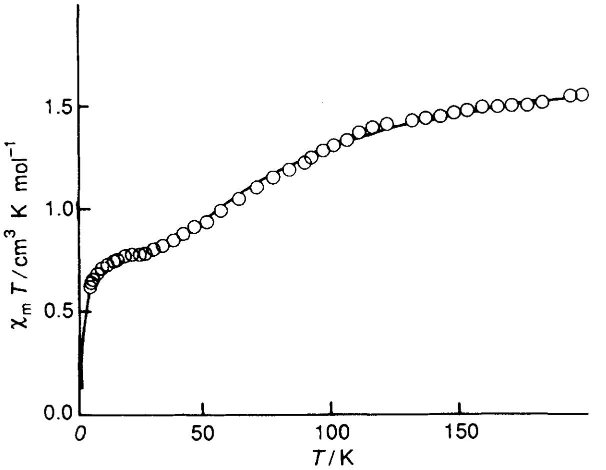

Figure 3. Product of susceptibility and temperature for [{Cu$_2$(terpy)Cl$_4$}$_2$] (○). Observed values (per mol of tetramer); (——) calculated curve using the parameters given in the text

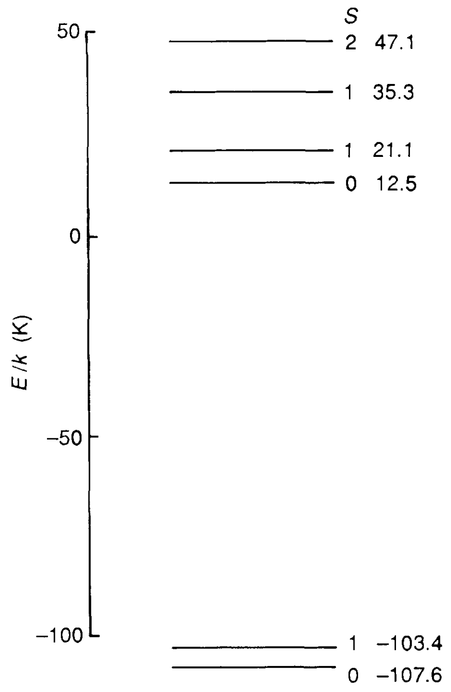

Figure 4. Order of the energy levels for [{Cu$_2$(terpy)Cl$_4$}$_2$] obtained from the analysis of the temperature dependence of the magnetic susceptibility

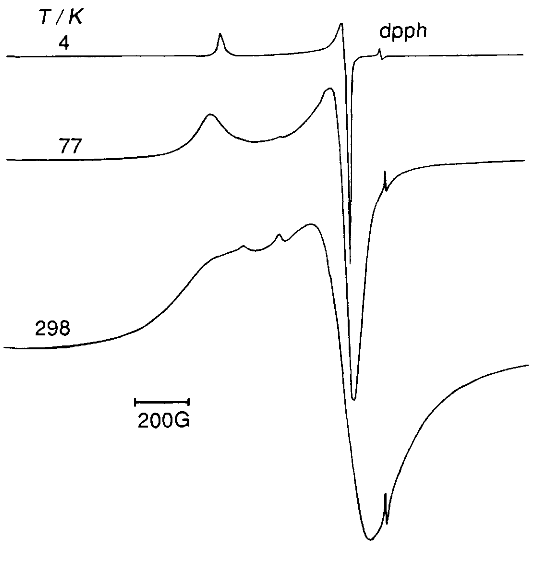

Figure 5. Q-band e.s.r. spectra of polycrystalline samples of [{Cu$_2$(terpy)Cl$_4$}$_2$] at selected temperatures. dpph = Diphenylpicrylhydrazyl; G = 10^{-4}T

Table 3. Magnetostructural data for [Cu$_2$Cl$_6$]$^{2-}$ dimers

	Cation	θ/°	σ/°	J/k(K)	Ref.
(1)	$\mathrm{C_4H_{10}NO^+}$	95.8	0.0	−44	12
(2)	$\mathrm{K^+}$	95.5	1.5	−28	13, 14
(3)	$\mathrm{H_2tatz^{2+}}$[a]	95.8	7.6	−28	12, 13
(4)	$\mathrm{NH_3Pr^{i+}}$	95.5	19.2	−14	13
(5)	$\mathrm{CH_2OHCH_2NH_3^+}$	95.9	20.0	−6	15
(6)	$\mathrm{H_2pipz^{2+}}$[b]	95.8	23.2	−13	14
(7)	$\mathrm{NH_2Me_2^+}$	95.6	23.6	15	13
(8)	$\mathrm{Hpip^+}$[c]	95.5	29.6	26	14
(9)	$\mathrm{Hbzpip^+}$[d]	95.3	28.7	30	13, 14
(10)	$\mathrm{MeNH_2C_2H_4Ph^+}$	95.1	46.1	70	15
(11)	$\mathrm{dbttf^+}$[e]	96.2	0.0	−67	12
(12)	$\mathrm{H_2tmen^{2+}}$[f]	96.4	17.9	−23	15
(13)	$\mathrm{H_2dmbipy^{2+}}$[g]	97.5	31.7	−19	13
(14)	[Cu(terpy)Cl]$^+$	97.0	12.4	−68	This work

[a] tatz = 2,4,6-Triamino-1,3,5-triazine. [b] pipz = Piperazine. [c] pip = Piperidine. [d] bzpip = 4-Benzylpiperidine. [e] dbttf = Dibenzyltetrathiafulvalene. [f] tmen = $NNN'N'$-Tetramethylethylenediamine. [g] dmbipy = 4,4′-Dimethylbipyridine.

(Figure 5). This feature must be due to $\Delta M_s = \pm 1$ transitions in the lowest triplet state, which is largely separated from the upper multiplet states, and apparently does not exhibit measurable zero-field splitting. Additionally, a very weak signal at 'half field' is observed in the X-band spectra, which is assigned to forbidden $\Delta M_s = 2$ transitions in the triplet state.

Two effects are observed when the temperature is increased: (*a*) the narrow axial signal becomes broader and, at room temperature, the two g components overlap in the X-band spectra and are only roughly distinguishable in the Q-band spectra, and (*b*) a narrower line with rhombic anisotropy is superimposed on the broad signal (Figure 5). The observation of temperature-dependent e.s.r. linewidths is not surprising since it is characteristic of exchange-coupled copper compounds and has been previously attributed to the phonon modulation of the spin anisotropies.[12,23] This fact leads to a J^4T dependence, thus broad linewidths are typical of strongly exchange-coupled copper salts. On the other hand, the intensity of the narrower signal depends on the sample preparation and increases with the sample agé. These facts lead us to think that this line corresponds to an impurity identified as CuCl$_2$·2H$_2$O. Similar impurity spectra have been observed previously for other hexachlorodicuprate(II) salts.[12] We have estimated the amount of this impurity from the room-temperature Q-band spectrum to be less than 1% in all samples.

Magnetostructural Correlations.—Since the present compound contains symmetrically dibridged Cu$_2$Cl$_6$ moieties, it is worthwhile examining magnetostructural correlations in a series of related systems. Table 3 and Figure 6 summarize the magnetic and structural data for these kinds of systems published up to date. It has been demonstrated that a general relationship exists between J and the bifold angle σ for a given bridging angle θ. As stated previously, each copper(II) atom in the Cu$_2$Cl$_6$ unit of [{Cu$_2$(terpy)Cl$_4$}$_2$] is in a '4 + 1' coordination mode leading to a slight bifold distortion that can be

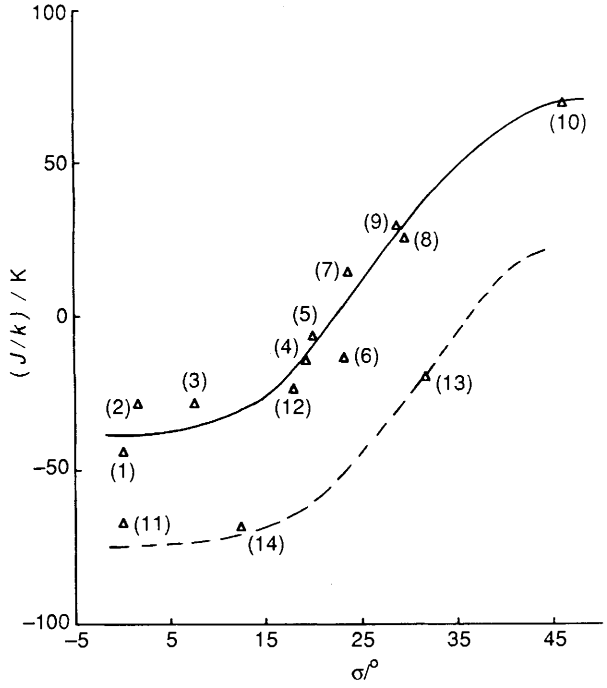

Figure 6. Plot of J/k *vs.* bifold angle (σ) for $[Cu_2Cl_6]^{2-}$ dimers. Solid and broken lines correspond to values of θ in the ranges 95.1—95.9 and 97.0—97.5° respectively, and they are drawn as a guide only

evaluated by a angle σ of 12.4°, whereas the bridging angle θ is 97.0°. As can be observed from Table 3 and Figure 6, the magnetic data in our case complement reported data and follow the expected trend: an increase of the bridging angle leads to an increase in the antiferromagnetic coupling, while the increase in σ, given a comparable bridging geometry, leads to increasingly ferromagnetic behaviour. In this context, complexes having θ in the range 95.1—95.9° are the most numerous and illustrate the above statements. Their behaviour is represented by the solid line drawn in Figure 6.[3–15] It is to be noted that for the doubly protonated salt $H_2dmbipy^{2+}$ and for the present compound the bridging angle is considerably larger (≈2°) and the exchange is expected to become more antiferromagnetic, and this is observed. We can now propose another relationship (broken line in Figure 6) correlating the salts with θ in the range 97.0—97.5°, which lies parallel to the former. Notwithstanding, it is clear that further magnetic and structural data for these kind of systems are required to delineate the full range of magneto-structural correlations.

Finally, if we look at the J_{12} value, it is similar to those found for the parallel square-planar chloride-bridged copper(II) dimers.[8] Although in our case the highly asymmetric Cu_2Cl_2 bridge cannot be directly compared to those systems, the low antiferromagnetic value of the exchange coupling is easily understood when the poor effective overlapping between the magnetic orbitals involved, essentially of $x^2 - y^2$ type, localized in the basal planes, is taken into account.

Acknowledgements

We thank the Comisión Asesora de Investigación en Ciencia y Tecnología for partial support of this research. J-V. F and P. G-R. thank the Generalitat Valenciana and the Spanish Ministerio de Educación y Ciencia, respectively, for a post-doctoral fellowship. F. S. thanks the Spanish Ministerio de Educación y Ciencia for a predoctoral fellowship. We thank Professor Dirk Reinen (Marburg) for making available the Varian E15 e.s.r. spectrometer. Diffraction data were collected at the Instituto Rocasolano (Consejo Superior de Investigaciones Cientificas), Madrid.

References

1 R. D. Willett, in 'Magneto-Structural Correlations in Exchange Coupled Systems,' eds. R. D. Willett, D. Gatteschi, and O. Kahn, NATO ASI Series, Plenum, New York, 1985, pp. 389—420; W. E. Hatfield, *ibid.*, pp. 555—602.

2 O. Kahn, *Angew. Chem., Int. Ed. Engl.*, 1985, **24**, 834.

3 J. V. Folgado, R. Ibáñez, E. Coronado, D. Beltrán-Porter, J. M. Savariault, and J. Galy, *Inorg. Chem.*, 1988, **27**, 19.

4 T. Rojo, M. I. Arriortua, J. L. Mesa, J. M. Savariault, G. Villeneuve, and D. Beltrán-Porter, *Inorg. Chem.*, 1988, **27**, 3904.

5 D. Beltrán-Porter, J. V. Folgado, R. Ibáñez, E. Coronado, J. L. Mesa, T. Rojo, and G. Villeneuve, in 'Organic and Inorganic Low Dimensional Crystalline Materials,' eds. M. Drillon and P. Delhaes, NATO-ASI Series, Plenum, New York, 1987, p. 433.

6 J. V. Folgado, E. Coronado, D. Beltrán-Porter, R. Burriel, A. Fuertes, and C. Miravitlles, *J. Chem. Soc., Dalton Trans.*, 1988, 3041.

7 J. V. Folgado, E. Coronado, D. Beltrán-Porter, T. Rojo, and A. Fuertes, *J. Chem. Soc., Dalton Trans.*, 1989, 237.

8 T. Rojo, M. I. Arriortua, J. Ruiz, J. Darriet, G. Villeneuve, and D. Beltrán-Porter, *J. Chem. Soc., Dalton Trans.*, 1987, 285.

9 T. Rojo, M. I. Arriortua, J. L. Mesa, R. Cortés, G. Villeneuve, and D. Beltrán-Porter, *Inorg. Chim. Acta*, 1987, **134**, 59.

10 J. V. Folgado, E. Coronado, and D. Beltrán-Porter, *J. Chem. Soc., Dalton Trans.*, 1986, 1061.

11 J. V. Folgado, E. Escrivá, A. Beltrán-Porter, and D. Beltrán-Porter, *Transition Met. Chem.* (*Weinheim, Ger.*), 1986, **11**, 485.

12 B. Scott, U. Geiser, R. D. Willett, B. Patyal, C. P. Landee, R. E. Greeney, T. Manfredini, G. C. Pellacani, A. B. Corradi, and L. P. Battaglia, *Inorg. Chem.*, 1988, **27**, 2454 and refs. therein.

13 S. O'Brien, R. M. Gaura, C. P. Landee, B. L. Ramakhrishna, and R. D. Willett, *Inorg. Chim. Acta*, 1988, **141**, 83 and refs. therein.

14 L. P. Battaglia, A. B. Corradi, U. Geiser, R. D. Willett, A. Motori, F. Sandrolini, L. Antolini, T. Manfredini, L. Menaube, and G. C. Pellacani, *J. Chem. Soc., Dalton Trans.*, 1988, 265 and refs. therein.

15 B. Scott and R. D. Willett, *Inorg. Chim. Acta*, 1988, **141**, 193 and refs. therein.

16 M. Honda, C. Katayama, J. Tanaka, and M. Tanaka, *Acta Crystallogr., Sect. C*, 1985, **41**, 197.

17 P. Main, G. Germain, and M. M. Woolfson, MULTAN 11/84, a system of computer programs for the automatic solution of crystal structures from *X*-ray diffraction data, Universities of York (England) and Louvain (Belgium), 1984.

18 G. M. Sheldrick, SHELX 76, program for crystal structure determination, Cambridge University, 1976.

19 'International Tables for *X*-Ray Crystallography,' Kynoch Press, Birmingham, 1974, vol. 4, pp. 72—99.

20 P. Roberts and G. M. Sheldrick, XANADU, program for crystallographic calculations, Cambridge University, 1975.

21 C. K. Johnson, ORTEP, Report ORNL-3794, Oak Ridge National Laboratory, Oak Ridge, Tennessee, 1965.

22 G. V. Rubenacker, J. E. Drumheller, K. Emerson, and R. D. Willett, *J. Magn. Magn. Mater.*, 1986, **54—57**, 1483.

23 U. Geiser, R. M. Gaura, R. D. Willett, and D. X. West, *Inorg. Chem.*, 1986, **25**, 4212.

Received 23*rd November* 1989; *Paper* 9/05019A